DETONATIONS OF LIQUID SPRAYS AND DROP SUSPENSIONS: EXPERIMENTS

S. M. Frolov
N. Semenov Institute of Chemical Physics, Moscow, Russia

Abstract
The paper is mainly focused on the experimental studies performed by the author's research group on direct detonation initiation and deflagration-to-detonation transition (DDT) in two-phase fuel drops – air mixtures. A particular attention is paid to the concept of fast DDT – a concept of controlled DDT with external stimulation of chemical activity in phase with a propagating shock wave.

1. Introduction
Detonability of liquid sprays and drop suspensions is currently a topic of growing interest mainly due to promising applications in novel air-breathing and rocket propulsion systems. Work on creating pulse detonation engines (PDE) is being carried out more and more actively [1]. Such engines will operate on a new principle of conversion of the chemical energy of fuel into propulsion: fuel will be burnt in traveling detonation waves. In comparison with existing combustion design in air-breathing and rocket engines, the detonation combustion of fuel in a traveling wave has a number of fundamental advantages. First, the thermodynamic efficiency of the detonation cycle is (theoretically) considerably higher than that of other cycles, especially at low pressures in the combustion chamber [1, 2]. Second, a PDE can burn both special fuels and conventional (liquid) jet propulsion fuels. Third, unlike many existing jet engines, a PDE has potentially a very simple design (requires no expensive compressors or turbopumps), reliable (has no moving elements), and self-sufficient (needs no boosters to reach the operation mode). Finally, using the multitube design of a PDE allows one to improve the thrust performance by simply increasing the number of combustion chambers. Inasmuch as the practical implementation of detonation combustion of fuel saves energy resources, stationary power plants operating on this principle are also being developed.

In a PDE, detonation is initiated in a tube that serves as the combustor. The detonation wave rapidly traverses the chamber resulting in a nearly constant-volume heat addition process that produces a high pressure in the combustor and provides the thrust. The operation of multitube PDE configurations at high detonation-initiation frequency (about 100 Hz and over) can produce a near-constant thrust. In order to use propagating detonations for propulsion and realize the PDE advantages mentioned above, a number of challenging fundamental and engineering problems has yet to be solved. These problems deal basically with low-cost achievement and control of successive detonations in a propulsion device. To ensure rapid development of a detonation wave, one needs to apply efficient liquid fuel injection and air supply systems to provide fast and nearly homogeneous mixing of the components in the detonation chamber and to reliably initiate a detonation at the shortests distances using the ignition sources with the lowest possible energy.

This paper is focused mainly on the experimental studies performed by the author's research group on direct detonation initiation and DDT in heterogeneous (drop) mixtures of liquid hydrocarbons in air relevant to PDE. Section 2 considers the experiments on direct detonation initiation in *n*-hexane and *n*-heptane sprays by electric discharges. Then, Section 3 describes the concept of fast DDT and provides several examples on DDT in *n*-hexane, *n*-heptane, aviation kerosene, and low-Octane-number gasoline sprays in air.

2. Direct initiation of heterogeneous detonations

2.1 General remarks

Both in practical applications and laboratory-scale experiments detonation in heterogeneous mixtures is usually initiated directly by a shock wave of a given strength, shape and duration. There exists the critical energy of the shock wave above which detonation in the tested two-phase mixture can be initiated, whereas lower energies are incapable of initiating detonation in two-phase mixtures. It is found from the analysis of the numerical solutions [3–6], that there exists a critical energy E_*, such that the explosion dynamics differs considerably for the explosion energy $E > E_*$ and $E < E_*$ (Fig. 1). Solid curves in Fig. 1 show the evolution of detonation wave in the case with $E > E_*$. In this case, after initiation the detonation wave attains a minimum propagation velocity $D_{\min} < D_{\mathrm{CJ}}$, where D_{CJ} is the steady detonation velocity. Then, after passing the minimum, the wave velocity starts to increase towards D_{CJ} 'from below.' Dashed curves in Fig. 1 show the case with $E < E_*$. Clearly, there exists a distance, corresponding to a certain shock radius, r_f^*, such that at $r_f > r_f^*$ the detonation wave decays. The value of r_f^* decreases with decreasing E. The magnitude of E_* depends on the ignition delay and fuel drop size.

Nonmonotonic behavior of unsteady detonation wave velocity is typical for all calculations. Detonation wave attains minimum velocity $D_{\min}$ at distance $\lambda_f = r_f / r_0 \approx \nu / 8$, where $r_0 = \left(E / \alpha_\nu p_0\right)^{1/\nu}$ is the dynamic radius, p_0 is the initial pressure, ν = 1, 2, and 3 for planar, cylindrical, and spherical symmetry, respectively, α_ν is the parameter of the blast model. The values of $D_{\min}$ decrease monotonically with decreasing point explosion energy and with increasing drop size in a fuel spray.

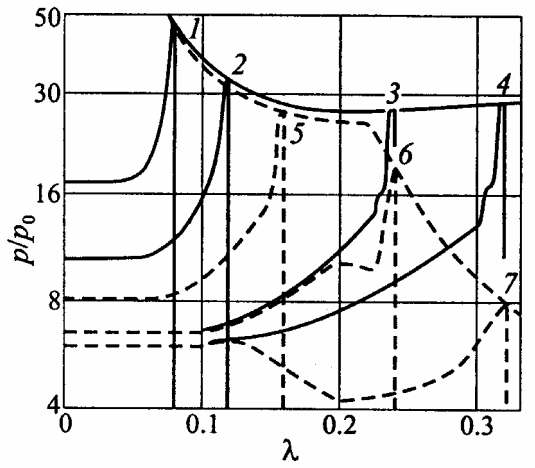

Figure 1: Predicted explosion dynamics under supercritical (solid curves) and subcritical (dashed curves) initiation of detonation in gas–drop suspension; $\lambda = r / r^0$ is the dimensionless distance; numbers correspond to different successive time instants [7]

Explosion of a fuel spray in gaseous oxidizer contains two independent parameters with the dimension of length: $r_0 = (E/p_0)^{1/\nu}$ and initial drop diameter d_0. In case of polydispersed sprays, drop diameter d_0 has the meaning of the Sauter mean diameter. To obtain the quantitative dependencies of the minimum velocity $D_{\min}$ of a nonsteady detonation wave on the governing parameters r_0, d_0, and ν in a two-phase medium, particular calculations were performed in [7] for spherical, cylindrical and plane geometries.

The analysis of numerical solutions for detonation initiation of monodispersed and polydispersed sprays of liquid fuels in air or oxygen with the initial drop diameter $d_0 = 50$–$700\ \mu$m showed, that the critical dynamic radius of direct detonation initiation (by an intense shock wave) is independent of the problem geometry, i.e.,

$$r^0(\nu) = \left(\frac{E_\nu}{p_0}\right)^{1/\nu} \approx const = r_c$$

where E_ν is the critical initiation energy relevant to symmetry index ν. Experimental data on initiating liquid hydrocarbon sprays in air by ball and cord charges of condensed explosive correlate well with this equation.

The constancy of r_c for different ν is not a strictly proved theoretical conclusion, but it is very useful for estimations. At known initiation energy for some spatial symmetry, it is possible to determine r_c and then the initiation energies for the other symmetry as

$$E_\nu \approx p_0 r_c^\nu$$

Another useful correlation obtained on the basis of numerical solutions is the ratio of r_c to the critical radius, $r_{c\nu}$, where detonation wave velocity attains its minimum:

$$r_{c\nu} \approx \frac{\nu r_c}{8}$$

With the help of the two latter equations, it is possible to express the initiation energies per unit area of the wave front at critical radius for different ν, as:

$$\frac{E_1}{2} = 0.5 p_0 r_c, \qquad \frac{E_2}{2\pi r_{c2}} = 0.5 p_0 r_c, \qquad \frac{E_3}{4\pi r_{c3}^2} = 0.57 p_0 r_c$$

These values turn out to be close to each other in all the three cases of symmetry.

Unfortunately, only a small portion of experimental data on detonations is related to initiation of heterogeneous systems with fuel drops. For example, in available experimental studies [8–10], heterogeneous drop detonations were initiated by a shock wave [8], gas detonation [9], or an explosive charge [10]. Moreover, the comparison of calculated results with experimental data can be performed only in few cases. For example, in [11], when initiating detonation of a cylindrical monodispersed spray of kerosene in oxygen (fuel drop size $d_0 = 400\ \mu$m) by an explosive charge, the value $E_2 \approx 0.34$ MJ/m was obtained. The experiments were performed in a sector shock tube at controlled fuel concentrations with the mixture equivalence ratio of 0.33. The calculated values for this case are $0.57 < E_2 < 0.75$ MJ/m. The correlation of calculated and experimental data for drop suspensions with the

Table 1: Predicted critical dynamic parameters of detonations in stoichiometric benzene–air drop suspensions depending on drop diameter [7]

Drop diameter μm	r_c M	E_1 MJ/m^2	E_2 MJ/m	E_3 MJ
0*	2.30	0.24	0.54	1.23
50	3.04	0.31	0.94	2.85
100	3.69	0.37	1.38	5.1
200	4.84	0.49	2.37	11.5
400	6.85	0.69	4.75	32.6
800	10.33	1.05	10.8	111.7
1000	11.94	1.21	14.4	172.4

*Zero diameter corresponds to vapor-phase composition

accuracy of a factor of about 2 should be considered as satisfactory, since the kinetic data for heterogeneous ignition exhibit considerable discrepancy.

Two basic points that follow from experimental studies of direct initiation of detonation in gaseous and two-phase mixtures should be emphasized. The first one is greater energies of detonation initiation in heterogeneous mixtures as compared to mixtures of the same fuel in the gaseous state. For example, the minimum energy of detonation initiation in a stoichiometric gaseous propane–air cloud is below 100 g TNT, whereas that for propane mist in air is about 200 g TNT [12]. In the absence of sufficient amounts of vapor phase, sprays of such fuels as kerosene, diesel fuel, and even gasoline larger than 100 μm fail to detonate in air, while these fuels dispersed to droplets 10 μm in diameter or prevaporized should have minimum energies of direct initiation of detonation comparable with those in gases. This observations are substantiated by calculations: Table 1 shows the predicted critical dynamic parameters (critical dynamic radius, r_c, and critical energies of detonation initiation, E_1, E_2, and E_3) of detonations in stoichiometric benzene–air drop suspensions depending on drop diameter [7].

The second point is that the relation between the minimum energies of initiation of detonation of heterogeneous mixtures in tubes and unconfined clouds obey the same relation, which follows from the Zel'dovich formula [13] $E_\nu = kL_{ind}^\nu$, where k is constant and L_{ind} is the induction zone length. This latter point is very important because it allows one to estimate the minimum energies of initiation of spherical detonation from simple measurements performed in tubes and thus avoid extremely expensive field experiments with large-scale clouds.

2.2 Experiments on direct detonation initiation

In [14, 15], two-phase *n*-hexane–air and *n*-heptane–air spray detonations were initiated by a powerful electric igniter mounted nearby the closed end of the detonation tube at a distance of 60 mm downstream from the atomizer (Fig. 2). The tube was 51 mm in diameter and 1.5 m long, and the fuel–air mixture was delivered continuously (during 1 s) into the tube through the air-assit atomizer mounted at the closed end.

The electric igniter was fed with a special high-voltage unit via a pulse generator and had a three-electrode scheme. The primary discharge had a fixed (57 J) energy (the energy E was estimated based on the rated capacity C and voltage U, i.e., $E = CU^2/2$). It produced

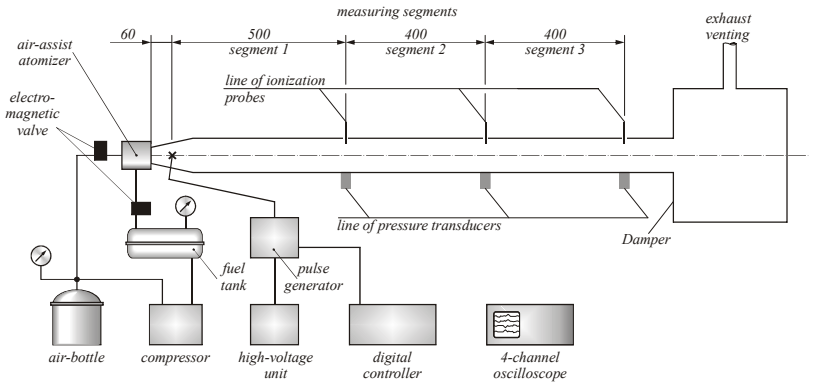

Figure 2: Sketch of the experimental setup [14, 15]

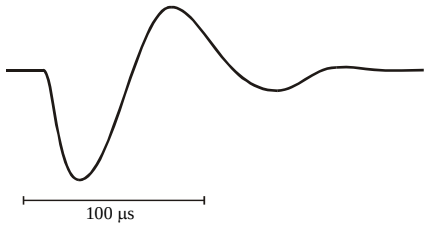

Figure 3: Discharge current measured by the Rogowsky coil mounted on the high-voltage cable. The signal was obtained at voltage 2500 V and rated capacitance 300 μF. The shape of current is close to sin wave with the oscillation period of 100 ± 10 μs

plasma to trigger the secondary discharge of a considerably higher energy. The capacitance of the secondary discharge was 600 μF. The characteristic time of the discharge produced by the igniter was about 100 μs as can be seen from Fig. 3. Figure 3 shows the discharge current measured by the Rogowsky coil mounted on the high-voltage cable 40 cm in length. The signal of Fig. 3 was obtained at the voltage of 2500 V and rated the capacitance of 300 μF. The shape of current is close to sin wave with the oscillation period of 100 ± 10 μs.

Figure 4 shows the schematics of two different atomizers used and the image of the spray issuing from the atomizer. The atomizers provided flow rates of air 12 (Fig. 4*a*) and 30 (Fig. 4*b*) liters per second, respectively.

Figure 5 demonstrates the express-method used for drop size measurements inside the experimental facility. The measurements were performed in situ by means of fast intrusion of thin (3 mm diameter) target rods through the spray across its centerline. The air-assist atomizer produced the fuel–air spray. At a specified distance L from the nozzle, a special guide tube was mounted so that it crossed normally the spray centerline. The guide tube had a narrow rectilinear slot to provide drop penetration inside the tube. The target rod was pushed by a spring mechanism through the guide tube. The rod had a processed cavity of rectilinear shape for detecting spray drops. The rod velocity was estimated based on the registered time of rod motion through the guide tube and the guide tube length. Two techniques for planar rod cavity preparation were used. In one, the rod cavity was first covered with a thick soot layer and then overcovered with a very thin layer of magnesium oxide (white smoke from burning magnesium powder). After hitting such a surface, fuel drops penetrated through the magnesium layer and exposed black spots on the white surface. The sizes of black spots were

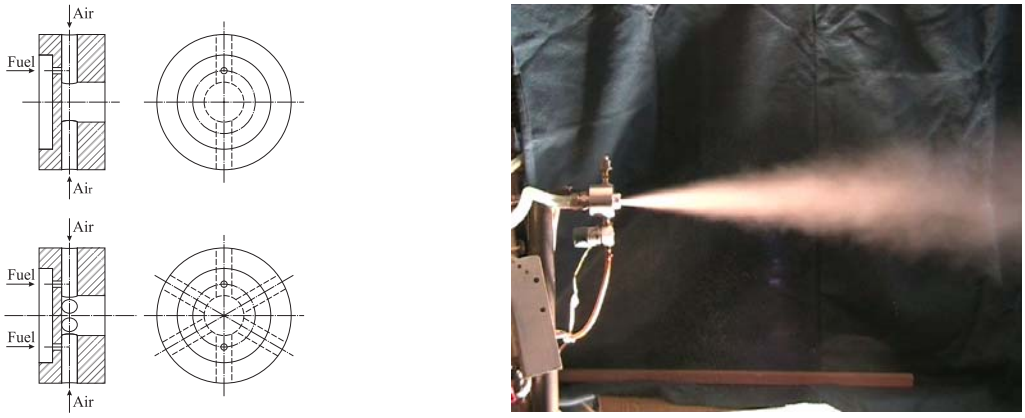

(*a*) (*b*)

Figure 4: Air-assist atomizers (*a*) and spray image (*b*). Air is supplied either via 2 or 6 radial channels. Liquid fuel is supplied via one or two axial channels into the air channel

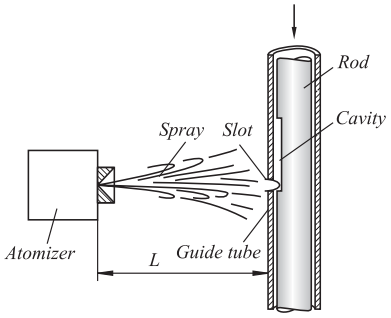

Figure 5: Schematic of the express-method used for drop size measurements. The measurements were performed by means of fast intrusion of thin target rods through the spray across its centerline attributed to drop sizes. The plates were examined with the use of optical microscope and drop size distributions were obtained.

Photographs in Figs. 6 show the examples of *n*-hexane spray signature. Presented here are the photographs of small portions of the surface. The scale of the photographs is such that the 150×100 mm photo corresponds approximately to the surface of 1000×670 μm size. At distance $L = 70$ mm from the nozzle there is evidently a dense spray with the dominating drop size considerably less than 10 μm. Relatively large light spots correspond to drop agglomerates. Also evident are elongated tracks produced by drops on the sooted surface due to tangential velocity. At distance $L = 100$ mm from the nozzle, the number of drops per unit volume decreases considerably both due to spray expansion and drop evaporation. This is clearly seen from drop size measurements at distance $L = 150$ mm: at this distance fuel drops still exist but their number is very small.

Figures 7 and 8 show the examples of measured drop size distributions in *n*-hexane (Fig. 7) and *n*-heptane (Fig. 8) sprays at $L = 70$ mm (Fig. 7*a*), 100 (Fig. 7*b* and 8*a*), and 150 mm (Figs. 7*c* and 8*b*). Drop size fractions plotted along *X*-axes have been chosen divisible to 5 μm. Size fraction of 5 μm corresponds to drops of size less than 5 μm, size fraction 10 μm corresponds to drops with size exceeding 5 μm and less than 10 μm, etc.

The air-assist atomizers generated very fine fuel sprays with most of drops having size less than 5 μm at $L = 70$ mm. At this distance, a very small fraction of drops had a character-

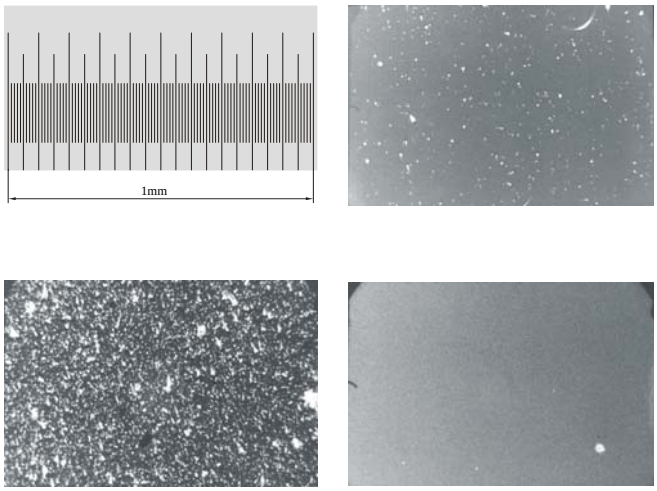

Figure 6: Photographs of *n*-hexane spray signature on the target rod surface: Upper left – scale of the photographs; bottom left – spray signature at distance 70 mm from the nozzle; upper right – spray signature at distance 100 mm from the nozzle; bottom right – spray signature at distance 150 mm from the nozzle

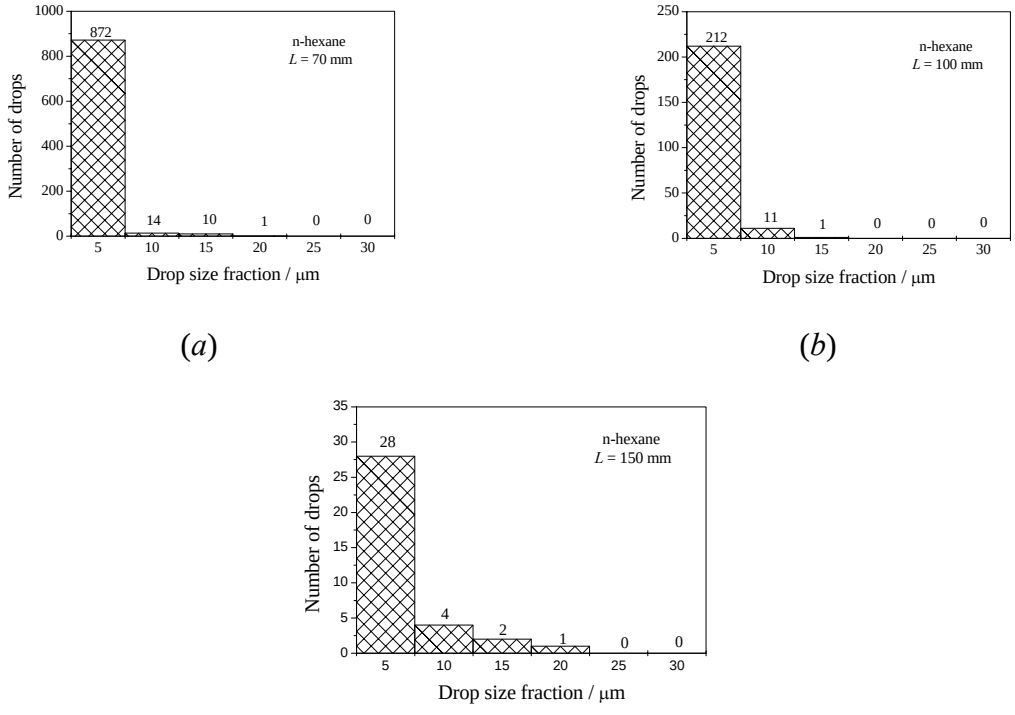

(*a*) (*b*)

(*c*)

Figure 7: Measured drop size distributions in *n*-hexane spray at $L = 70$ mm (*a*), 100 (*b*), and 150 mm (*c*). Drop size fractions plotted along *X*-axes are chosen divisible to 5 μm. Size fraction of 5 μm corresponds to drops of size less than 5 μm, size fraction 10 μm corresponds to drops with size exceeding 5 μm and less than 10 μm, etc.

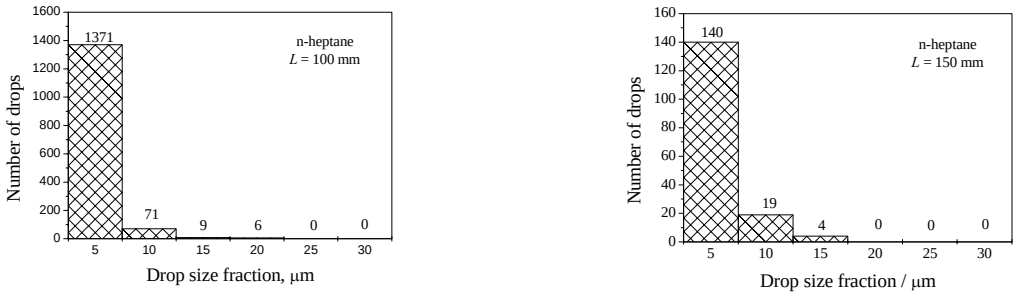

(*a*) (*b*)

Figure 8: Measured drop size distributions in *n*-heptane spray at $L = 100$ mm (*a*) and 150 mm (*b*)

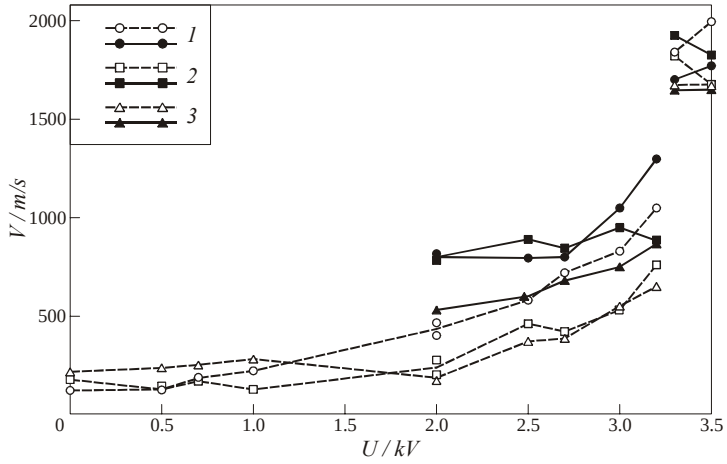

Figure 9: Measured shock wave (solid curves) and flame front (dashed curves) velocities vs. igniter voltage (*n*-hexane) at different measuring segments (*1* to *3*). Due to poor accuracy of pressure measurements at low ignition energies, measurements of shock wave velocity were performed beginning from the voltage of 2000 V

istic size exceeding 5 μm. The distance required for almost complete evaporation of fuel spray depended on the fuel type: *n*-hexane sprays evaporated at distances of about 100–150 mm, *n*-heptane sprays evaporated at distances of about 200–250 mm. Additional experiments with whitespirit sprays indicated that such sprays did not evaporate considerably at a length-scale of the entire experimental setup (1500 mm). Thus, at the location of igniter (60 mm from the atomizer nozzle) the fuel–air mixtures were essentially two-phase.

In the experiments on direct detonation initiation, the equivalence ratio of the fuel-air mixture averaged over the experimental run based on the air and fuel consumption was estimated as 1.2 ± 0.1. To measure the propagation velocity of shock waves and flames, pressure transducers and ionization probes were installed in tree cross-sections of the tube at a distance of 500, 900, and 1300 mm from the discharge electrodes. Figure 9 summarizes the results of experiments for *n*-hexane with different voltage at the discharge electrodes. It follows from from Figs. 9 and 10 that increase in voltage to 2000 V exerts almost no effect on the flame propagation velocity. As the voltage exceeded 3300 V, a detonation wave was observed at all measuring segments (Fig. 11). In other words, as the ignition energy exceeded

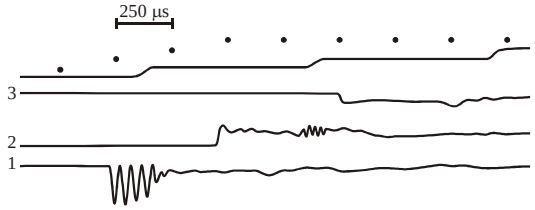

Figure 10: Records of ionization current (upper record with time markers) and pressure at measuring stations 1, 2, and 3 at the ignition energy of 3130 J in the *n*-hexane spray. All ionization gauges were connected to one measuring circuit and thus continuously contributed to the upper signal: steps on the signal correspond to flame arrival at successive measuring stations. The comparison of the pressure and ionization gauge records at the corresponding measuring stations indicates that the shock wave was always ahead of the flame front

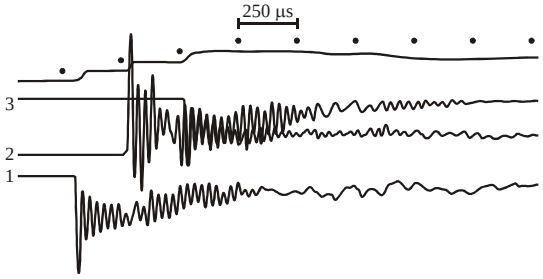

Figure 11: Records of ionization current (upper beam with time markers) and pressure at measuring stations 1, 2, and 3 at the ignition energy of 3324 J in the *n*-hexane spray. The pressure and ionization gauge records at the corresponding measuring stations indicate simultaneous arrival of a shock wave and flame front

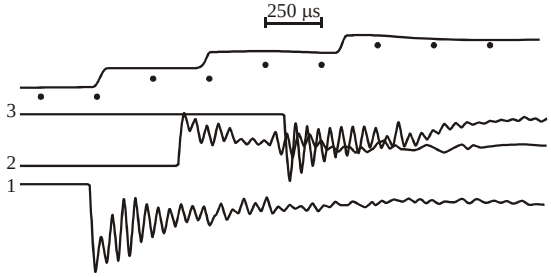

Figure 12: Records of ionization current (upper beam with time markers) and pressure at measuring stations 1, 2, and 3 at the ignition energy of 3324 J in the *n*-heptane spray. The comparison of pressure and ionization gauge records at the corresponding measuring stations indicates that flame lags behind the lead shock wave in this run

3.3 kJ, direct initiation of detonation in *n*-hexane spray has been obtained. A similar set of experiments was performed for *n*-heptane. In the test with the discharge voltage of 3300 V, *n*-heptane spray did not detonate (Fig. 12). Increase of the ignition energy from 3.3 to 3.7 kJ resulted in direct detonation initiation in *n*-heptane spray.

Figure 13 summarizes the results of experiments for *n*-heptane with different igniter voltage. Again, dashed and solid curves correspond to the measured flame and shock wave velocities, respectively, at the corresponding measuring segments (denoted by numbers *1*, *2*,

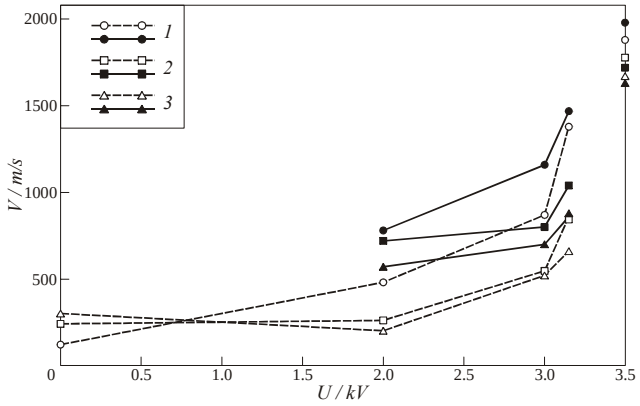

Figure 13: Measured shock wave (solid curves) and flame front (dashed curves) velocities vs. igniter voltage for the *n*-heptane spray at different measuring segments (*1* to *3*). Due to poor accuracy of pressure measurements at low ignition energies, the measurements of the shock wave velocity were performed started from the voltage of 2000 V

and *3*). Similar to Fig. 9, increase in the igniter voltage from 0 to 2000 V exerts almost no effect on the *n*-heptane flame propagation velocity at segments *2* and *3*. Contrary to flame behavior at these measuring segments, flame velocity at segment *1* gradually increases with voltage. At voltage exceeding 3500 V, a detonation wave appears at all measuring segments *1* to 3. Thus, the critical energy for direct detonation initiation in *n*-heptane spray was found to be about 3.7 kJ. Note that both atomizers shown in Fig. 4 provided almost similar conditions for detonation initiation in n-hexane and *n*-heptane sprays.

Further experimental studies of direct initiation of *n*-hexane spray detonation in air have been reported in [16, 17]. In these papers, the effect of tube diameter on the critical detonation initiation energy has been investigated. In addition to tube 51 mm in diameter, two other tubes of diameter 36 and 28 mm were used. As compared to the experiments described above, the igniter configuration was modified to decrease the initiation energy of detonation in the 51-millimeter-diameter tube from 3.3 kJ (as in Fig. 8) to 1.5 kJ. Such a decrease became possible due to shortening the characteristic time of energy deposition in the discharge from 100 μs to 40 μs. Figure 14 shows the measured shock wave and flame front velocities vs. discharge voltage for *n*-hexane–air sprays in tubes of different diameters: 51 (*a*) and 28 mm (*b*).

As follows from Fig. 14, a decrease in the tube diameter results in diminishing the critical detonation initiation energy. Thus, almost two-fold decrease in tube diameter (from 51 to 28 mm) resulted in decreasing the critical initiation energy from 1.5 to 0.82 kJ, i.e., almost two-fold. In a small-diameter tube, the minimal voltage required for detonation initiation has decreased from 2100 V in Fig. 14*a* to about 1600 V in Fig. 14*b*. At small (near-limit) tube diameter of 28 mm, there is no abrupt change in wave velocity with increasing the initiator energy.

In [14, 15], interesting experiments on detonation initiation by two successively triggered electrical discharges were reported. In the setup of Fig. 3 an additional (second) electric igniter was mounted at a certain distance (100 to 300 mm) from the main (first) electric igniter (Fig. 15). The experimental procedure encountered a number of steps dealing with "tuning" a specially designed controller in terms of a preset delay time (time τ in Fig. 16) for triggering the second igniter. The aim of "tuning" was to obtain the direct detonation initiation at the lowest possible total ignition energy.

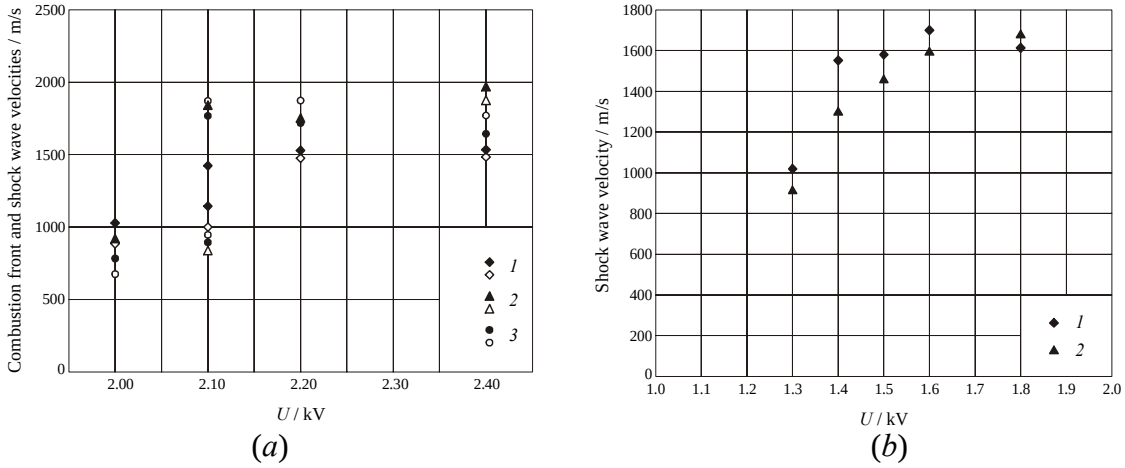

Figure 14: Measured shock wave (solid symbols) and flame front (open symbols) velocities as a function of discharge voltage for *n*-hexane sprays in air in tubes of different inner diameter: 51 mm (*a*) and 28 mm (*b*). Numbers *1* to *3* denote the measuring stations located at 500, 900, and 1300 mm (*a*) and 125, 525, and 925 mm (*b*) from the discharge [16, 17]

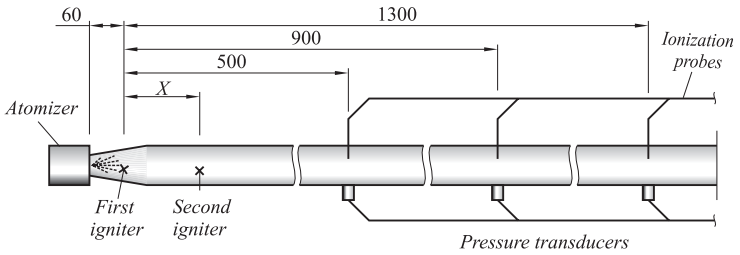

Figure 15: Schematic of the test tube with air-assist atomizer, two igniters, line of pressure transducers, and line of ionization probes; X is the distance between successively triggered igniters

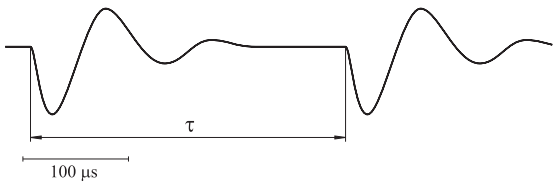

Figure 16: Discharge current in a two-discharge circuit measured by the Rogowsky coil mounted on the high-voltage cable. The signal was obtained at voltage 2500 V and rated capacitance 300 μF for each discharge. The second igniter was triggered 300 μs after the first igniter

The "tuning" procedure was as follows. After triggering the first igniter, the blast wave arrival time at location of the second igniter was measured by using a signal of pressure transducer installed at $X = 100$ mm. As the blast wave at this tube section had a smeared rather than sharp front, the arrival times of the lead and the rear front portions were detected. Thus, the shock arrival time at the location of the second igniter was represented by two curves at the "voltage vs. triggering delay time" plane, as curves *1* and *2* in Fig. 17. Plotted

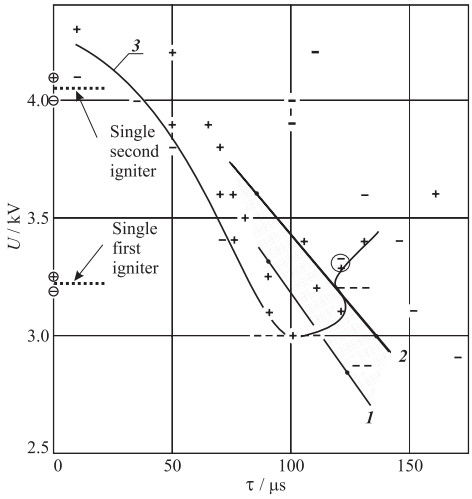

Figure 17: Results of experiments on initiation of *n*-hexane spray detonation by two successively triggered igniters mounted at a distance of 100 mm from each other. Plus and minus signs correspond to reliable "go" and "no go" detonation conditions. Plus-minus sign in the circle corresponds to marginal detonation that is not reliably reproduced in a series of similar experiments. The solid curve separates plus and minus signs and interpolates the conditions required for detonation initiation. Shaded area between lines *1* and *2* corresponds to the arrival time of initial shock at location of lateral igniter

along the *X*-axis in Fig. 17 is the delay time τ of triggering the second igniter. Plotted along the *Y*-axis is the voltage at high-voltage blocks of the igniters. It follows from analyzing the distance between curves *1* and *2* (along the τ-axis) that the width of the blast wave at $X = 100$ mm is 15–25 μs. The starting voltage for the first igniter was varied from 4400 to 2800 V. Based on these measurements, a first approximation for the time delay of triggering the second igniter was obtained for the next run. This time delay was preset in the controller. The next run encountered time-delayed triggering of both first and second igniter. Blast wave velocity at segments *2* and *3* was then measured at this preset value of the triggering time. In the subsequent runs, the time delay of ignition triggering was varied in a certain vicinity of this value to reveal the best conditions for blast wave amplification to a detonation. Then the voltage was decreased and a new test series at a lower total ignition energy was performed. At each stage of the procedure, several runs were performed to collect the statistics on the reproducibility of the results. It has been found that the results were satisfactorily reproducible.

Figure 18 summarizes the results of experiments for *n*-hexane sprays and a distance of 200 mm between the igniters. The delay time of triggering the second igniter (counted from the activation of the first igniter), and the voltage at high voltage blocks of the igniters are plotted along *X* and *Y* axes, respectively. Plus and minus signs correspond to reliable "go" and "no go" detonation conditions at measuring stations *2* and *3* reproduced in several similar experiments. It follows from Fig. 18 that there exist resonant conditions for triggering the second igniter in terms of the delay time. The "width"of the detonation peninsula is about 50 μs at 3000 V and 10 μs at 2500 V. At a fixed delay time, e.g., 270 μs, a detonation arises at 2500 V and does not arise at a higher voltage (2600 to 2900 V) that indicates the necessity of careful synchronization of the second igniter triggering with the blast wave generated by the first igniter.

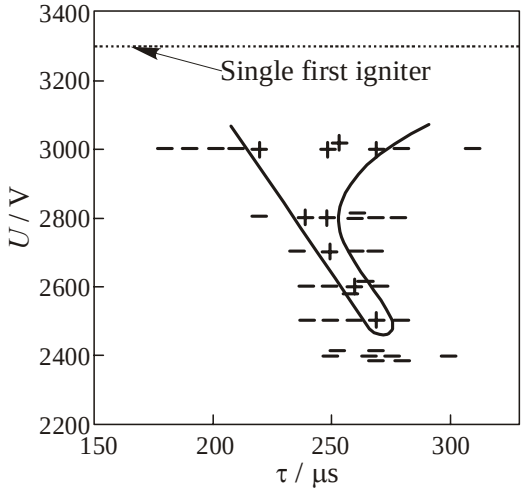

Figure 18: Detonation initiation energy (in terms of voltage U applied to the high-voltage blocks of two igniters with similar capacity of 300 μF) vs. the delay time τ of triggering the second igniter (counted from activation of first igniter) [14, 15]

The lowest voltage required for detonation initiation with two successively triggered igniters was 2500 instead of 3300 V required with a single igniter. This decrease in voltage indicates almost two-fold decrease in the total initiation energy. Thus, the findings of [14, 15] indicate that (*i*) there exist resonant conditions for successive triggering of two igniters that have to be met in order to initiate detonation; (*ii*) the minimal total initiation energy by successively triggered igniters is lower than that required for direct detonation initiation by a single igniter; and (*iii*) the detonation peninsula at the "initiation energy vs. triggering time delay" plane is very narrow and indicates the necessity of careful synchronization of successive discharge triggering.

3. Deflagration-to-detonation transition in two-phase mixtures

3.1 General remarks

The classic mechanism of DDT in a straight smooth tube includes several stages [18, 19], namely, (1) forced mixture ignition with the formation of a laminar flame, (2) progressing increase in the rate of combustion because of the appearance of instabilities and subsequently turbulent flow ahead of the flame front, (3) shock wave formation and strengthening ahead of the accelerating flame front, and (4) self-ignition of the shock-compressed mixture in the region between the shock wave and flame front [20] ("explosion in the explosion" [21]) resulting in the formation of an overdriven detonation wave and then (5) self-sustaining Chapman–Jouguet detonation. The time and distance of the DDT are known to be largely determined by the first three stages [22]. Detonation in air mixtures of hydrocarbon fuels requires that the "visible" velocity of the turbulent flame front in the laboratory coordinate system be higher than 1000 m/s [23]. At such a flame front velocity, the shock wave running ahead has a velocity higher than 1300 m/s (the shock wave Mach number is $M \sim 3.8$), and the pressure and temperature of the explosive mixture behind it are higher than 1.7 MPa and 1200 K, respectively.

In our recent works [24–27, 15] and reviews [28, 29], a new method for obtaining detonation in a straight smooth tube was suggested. Its essence is the forced acceleration of a comparatively weak shock wave running before the flame front to intensities sufficient for the

formation of a detonation. For this purpose, distributed igniters were mounted along a straight smooth tube. To exclude the first three poorly reproducible DDT stages from consideration, the primary shock wave was obtained using either an electric discharge [24–28] or a tube section with a Shchelkin spiral [17, 29]. The shock wave obtained was accelerated by switching on each ignition source as the wave arrived at the corresponding tube section. In other words, the shock wave was accelerated by providing fast forced explosive mixture ignition in the nearest vicinity of the running shock front. This technique allowed a detonation to be initiated at a distance and in a time much smaller compared with the classic DDT. In experiments [24–28] with detonation initiation, the mismatch between the arrival of the shock wave and gas ignition did not exceed 100 μs. At a larger mismatch, the other conditions being equal, no detonation occurred. Interestingly, the admissible mismatch value is comparable with the characteristic reaction time in the detonation wave at the limit of detonation [30].

In [24–28], the detonation of a stoichiometric propane–air mixture was obtained in a tube 51 mm in diameter at the initial shock wave velocity at a level of 800–1000 m/s (the shock wave Mach number was M ~2.4–3.0). Note that, for the formation of a similar shock wave ahead of a flame front, the flame front should be accelerated to a visible velocity of about 550–750 m/s. This velocity is much lower than the velocity of the flame required for the spontaneous DDT (~1000 m/s). It follows that the length and time of the DDT can be reduced substantially by providing the possibility of forced shock wave acceleration before the flame front; that is, one can then obtain a “fast” DDT. Further, the fast DDT will be understood as the appearance of detonation in a fuel–air mixture when a turbulent flame is accelerated to a velocity much lower than the velocity required for the classic DDT in a straight tube. In [28], the classic DDT was called “slow” to distinguish it from the fast DDT. The new technique for initiating detonation studied in [24–28] was called in [24] “detonation initiation by a running forced ignition pulse.”

Let us turn from DDT in a straight smooth tube to DDT in a tube with regular obstacles [19, 31]. The mechanism of DDT in such tubes is in many respects similar to the mechanism [18–22] described above. There are also important differences. First, the flame is accelerated much more quickly in a tube with obstacles because of the additional turbulizing of a fresh explosive mixture when it flows around obstacles. Secondly, there appear new possibilities for gas ignition. A gas can be selfignited in the reflection of the shock wave from an obstacle or (if obstacles are large) because of mixing of directed jets of hot combustion products with a cold fresh mixture.

The possibility of the local self-ignition of a fresh mixture caused by shock wave reflection from an obstacle suggests an idea [28] that, in DDT in tubes with obstacles, not only the classic scenario [18–22], but also the scenario of detonation initiation by a running ignition pulse, however spontaneous rather than forced, is possible. Gas ignition in the vicinity of the shock wave running in front of the flame then occurs because of the self-ignition of the substance compressed by the shock wave reflected from obstacles rather than because of external stimulation of chemical activity. In other words, DDT in tubes with obstacles includes a stage at which fast detonation initiation by a running spontaneous ignition pulse (fast DDT) is possible in principle. As with forced ignition experiments [24–28], the possibility of fast DDT is then determined by the degree to which the time instants of the arrival of the shock wave at one or another tube cross section and gas ignition in the section coincide. In the case under consideration, we must compare the moment of the arrival of the shock wave at an obstacle and the moment of gas self-ignition behind the reflected wave. The latter is, as is well known, characterized by ignition delay.

Ignition delay depends on the composition of the mixture, the intensity of the running shock wave, and the duration of the compression phase in it. We assume that the admissible self-ignition delay time is less than 100 μs at the normal reflection of a long shock wave from obstacles. Fast DDT in a stoichiometric propane–air mixture then requires a shock wave running at a velocity of 950–970 m/s (the shock wave Mach number is $M \sim 2.8$) [32]. During DDT, such a wave is formed in front of the flame propagating at a velocity of about 700 m/s. The pressure and temperature in the reflection of such a shock wave from an obstacle are approximately 4.5 MPa and 1300 K. The obtained shock wave velocity value is within the range of shock wave velocities used in experiments [24–28] with the initiation of detonation by a running forced ignition pulse. It follows that there are no prerequisites for fast DDT when the visible flame velocity in the stoichiometric propane–air mixture is still lower than ~700 m/s. At this stage of flame development, progressing turbulent flame acceleration occurs and the shock wave is strengthened because of interaction with compression waves generated by the flame and separate ignition zones in the vicinity of obstacles. When the velocity of the flame exceeds 700 m/s and the velocity of the shock wave before the flame front exceeds ~950–970 m/s, fast DDT becomes possible theoretically. Note that the above estimates ignored effects related to explosive mixture expansion in rarefaction waves inevitable in the diffraction of shock waves by obstacles. These effects depending on the shape of obstacles increase ignition delays and, therefore, increase the threshold flame velocity required for fast DDT.

In view of the possibility in principle of fast DDT, fundamental questions concerning the conditions of their occurrence and methods for preventing them arise. Below, we provide several examples of fast DDT in heterogeneous fuel–air mixtures under conditions when distributed self-ignition zones spontaneously form in a flow behind a running shock wave.

3.2 Experiments on DDT

Unlike the DDT in gaseous mixtures, the DDT in drop mixtures of liquid fuel with air (oxygen) is virtually unstudied. In the past, there were only few publications relevant to DDT processes in suspensions of liquid droplets in oxygen. Webber [33] was, probably, the first to observe amplification of weak shock waves in the course of their propagation through burning sprays, that is, to indicate that there was some mechanism which could be responsible for DDT in sprays. More comprehensive studies [34, 35] have demonstrated that transition to detonation within short distances in burning sprays is feasible. A mandatory condition for this transition is a weak shock wave that must be sent into a burning spray or spray to be ignited. The study also indicated definitely that it is droplet breakup that is responsible for shock wave amplification. In drop mixtures of liquid fuel with gaseous oxygen, a deflagration-to-detonation transition was observed by Pierce and Nicholls [36], who reported that the predetonation distance was 20–100 tube diameters long.

The first experimental observations of DDT in drop mixtures of *n*-hexane and *n*-heptane with air were apparently reported by us in [37, 29]. The studies in [37, 29] continued the studies described above in Section 2. To decrease the detonation initiation energy as compared with that obtained at direct initiation, we performed experiments in tubes of smaller diameters (36 and 28 mm). In addition, to enhance the turbulence in the jet of the drop mixture coming from the atomizer, a 600-mm long Shchelkin spiral wound from a steel wire 4 mm in diameter at a spiral pitch of 18 mm was placed in the tube (Fig. 19). At a low ignition energy of 130–240 J, the velocity of the shock wave leaving the spiral reached 900–1000 m/s (Figs. 20*a* and 20*b*). A change in the spiral wire diameter or in the spiral pitch or

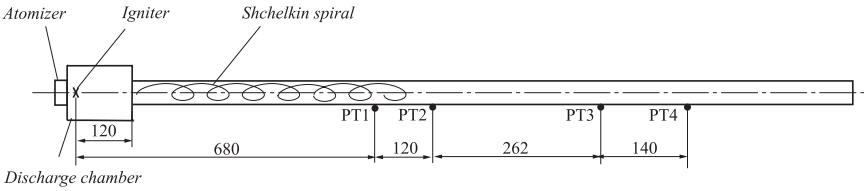

Figure 19: Schematic of a straight explosion tube 36 mm in diameter with air-assist atomizer, igniter, discharge chamber, Shchelkin spiral, and pressure transducers PT1 to PT4

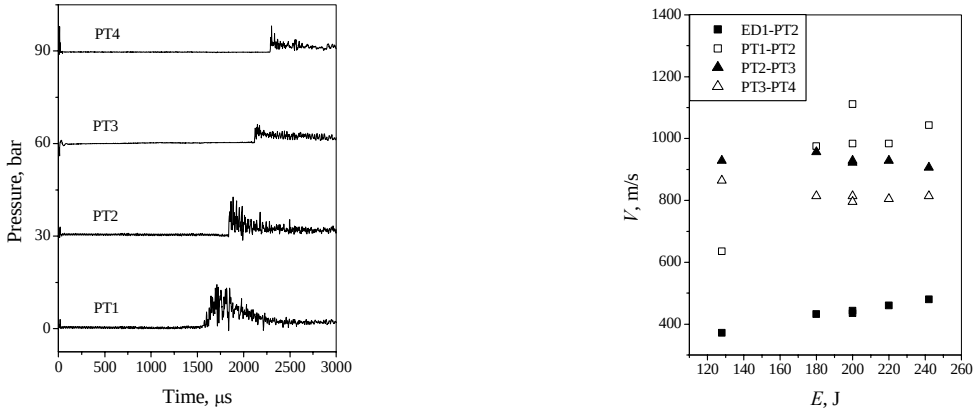

(*a*) (*b*)

Figure 20: Pressure profiles recorded by transducers PT1–PT4 in an experiment with an ignition energy of E = 128 J (*a*), and the measured shock wave velocity in a drop *n*-hexane–air mixture over different measurement segments vs. ignition energy (*b*)

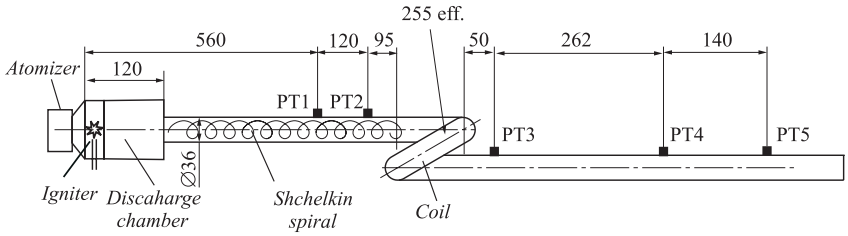

Figure 21: Schematic of an explosion tube 36 mm in diameter with a coil

length did not lead to any significant changes in the characteristics of the obtained shock waves at such ignition energies.

To further enhance the obtained shock wave, a new element—a coil of a tube—was placed downstream of the section with the Shchelkin spiral. Figure 21 presents a schematic of the explosion tube 36 mm in diameter with air-assist atomizer, discharge chamber, electric igniter, Shchelkin spiral, and tube coil. Piezoelectric pressure transducers PT1–PT5 were used to record the profiles of pressure waves in the tube and to determine the velocities of these waves. We expected that the curvilinear reflecting surfaces in coil might lead to gas-dynamic "focusing" of a shock wave and to a fast DDT.

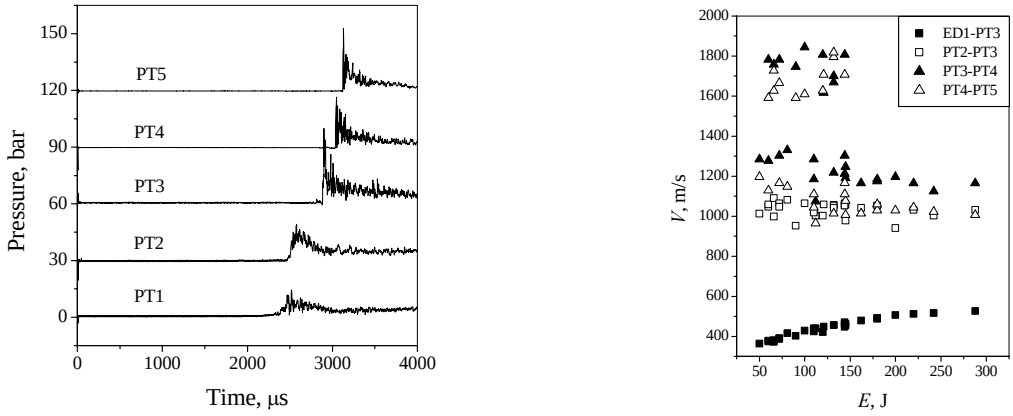

(*a*) (*b*)

Figure 22: Pressure profiles recorded by transducers PT1–PT5 in an experiment with an ignition energy of E = 60 J (*a*), and the measured shock wave velocity in a drop *n*-hexane–air mixture over different measurement segments vs. ignition energy (*b*).

Figure 22*a* shows the pressure profiles recorded by transducers PT1–PT5 in an experiment with an ignition energy of E = 60 J. Unlike experiments in a straight tube, here, transducer PT3 at the outlet of the coil detected a detonation wave. The detonation emerged within the coil at a distance of about 1 m from the discharger (about 28 tube diameters). The detonation wave propagated to the end of the tube at a velocity of 1750±20 m/s. Figure 22*b* presents the results of measuring the velocity V of pressure waves in this set of experiments over four measuring segments: between the igniter and transducer PT3 (ED–PT3), between transducers PT2 and PT3 (PT2–PT3), between transducers PT3 and PT4 (PT3–PT4), and between transducers PT4 and PT5 (PT4–PT5). It is seen that, at ignition energies from 60 to 144 J, a number of experiments detected detonation at the outlet of the coil. Detonation occurred randomly with a frequency of about 50%. It is of interest that detonation never emerged at higher ignition energies (144–300 J). Probably, this is because a cumulating pressure wave (in the terms of Shchelkin) was formed outside of the coil at higher ignition energies.

To further decrease the ignition energy sufficient for fast DDT within the coil, we used the tube of a smaller diameter, 28 mm. Figure 23 presents a schematic of an experimental setup in which the minimal energy (30 J) of detonation initiation in drop *n*-hexane–air mixtures was attained. The setup consisted of atomizer, discharge chamber, electric igniter, Shchelkin spiral, tube coil, ionization probe, two tapered sections, and main tube of a diameter of 51 mm. The pressure profiles recorded on this setup (Fig. 24*a*) show that detonation emerged within the coil and propagated into the tube 41 mm in diameter and then into the main tube. At ignition energies from 30 to 50 J, DDT in the coil always occurred and the arising detonation propagated into the main tube (Fig. 22*a*). At ignition energies from 50 to 130 J, detonation did not always propagate into the main tube. At ignition energies from 130 to 300 J, no detonation was observed. Similar results were obtained for drop *n*-heptane–air mixtures [37, 29].

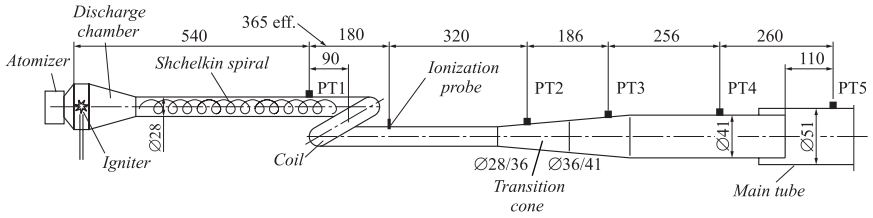

Figure 23: Schematic of an explosion tube 28 mm in diameter with a coil and a transition section to a tube 51 mm in diameter

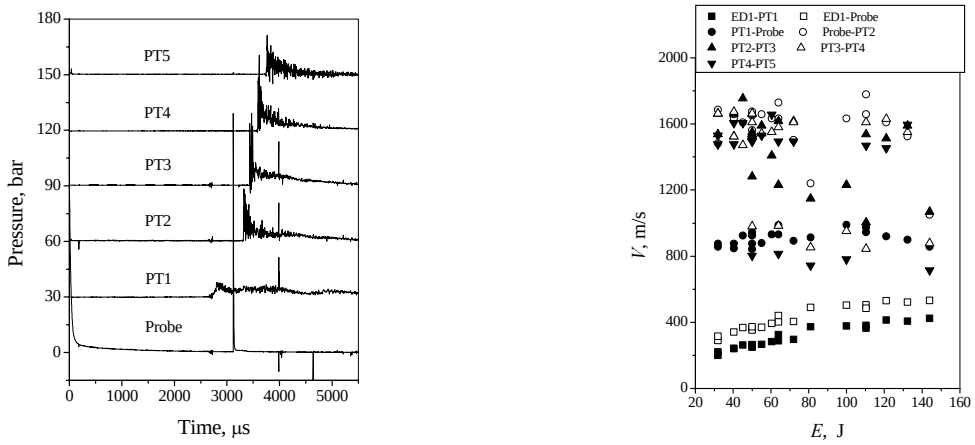

(*a*) (*b*)

Figure 24: Pressure profiles recorded by transducers PT1–PT5 in an experiment with an ignition energy of E = 32 J (*a*), and the measured shock wave velocity in a drop *n*-hexane–air mixture over different measurement segments vs. ignition energy (*b*).

Design changes in the setup shown in Fig. 23 (changes in the shape of discharge chamber *2*, the length of spiral, the shape of coil, the length of the section of the tube from the end of the spiral to the coil, or even the length of the section of the tube to the tapered sections) led to changes in the observed explosion dynamics. A high reproducibility of experiments on detonation initiation in the coil became possible owing to careful optimization of the setup design.

Thus, the replacement of the straight explosion tube 51 mm in diameter (see Fig. 2) by the curved tube of Fig. 23 decreased the detonation initiation energy of drop *n*-hexane–air and *n*-heptane–air mixtures by two orders of magnitude: from 3300–3700 to 30 J. In the experiments with the coil, an electric discharge was used as a source of ignition of a mixture rather than a source of a strong initiating shock wave. Consequently, in these experiments we detected a fast DDT in drop mixtures of hydrocarbon fuels with air. The detonation run-up distance in the tube 28 mm in diameter turned out to be close to 1 m, i.e., to 36 tube diameters, and the total predetonation distance to the main tube 51 mm in diameter was 1.8 m. For comparison, we note that a DDT in a gaseous propane–air mixture requires no less than 260 diameters for a straight smooth tube and more than 60 diameters for a straight tube with turbulence promoters in the form of regular obstacles [27].

In [38], the experiments on DDT in drop mixtures of aviation kerosene with air were reported. Low detonability of jet propulsion kerosene in air is the key barrier for the progress in the development of air-breathing PDE. In view of it, arranging of fast DDT seems to be a promising solution. As a matter of fact, our experimental studies described below demonstrate that the use of the fast DDT concept allows one to initiate a detonation of jet propulsion kerosene TS-1 (Russian analog of Jet-A) at short run-up distance and time applying a very small ignition energy.

Figure 25 shows the experimental setup, comprising injector *1*, detonation tube *2*, igniter *3*, pressure transducers *4*, detonation arrester *5*, air bottle *6*, fuel valve *7*, air compressor *8*, kerosene tank *9*, fuel filter *10*, digital controller *11*, power supply *12*, PC *13*, control relay *14*, prevaporizer *15* (insert *A*), thermostat *16*, electrical heaters *17* and *18*, and thermocouples *19*. The fuel and air supply system provided the supply of fuel mixture components in constant proportion due to the same driving pressure. Mixing of fuel and air started in the air-assist atomizer and terminated in the detonation tube of internal diameter 51 mm and 3 m long. The air-assist atomizer provided very fine kerosene drops 5 to 10 μm in diameter. The two-phase fuel–air mixture was continuously injected to the prevaporizer section *15* of the detonation tube. In this section, kerosene drops were partly vaporized and the hybrid drop–vapor–air mixture followed to the tube section with Shchelkin spiral (insert *B*) and a removable 2-coil tube segment (insert *C*).

Two sets of experiments have been made. In the first set, the detonation tube was straight, while in the second it contained a 2-coil tube segment. The length of the Shchelkin spiral in both detonation tubes was 800 mm. The spiral was mounted 70 mm downstream from the prevaporizer nozzle. In the experiments with both tubes, the prevaporizer wall temperature was 190 ± 10^{o}C. The temperature of the tube segment with the Shchelkin spiral

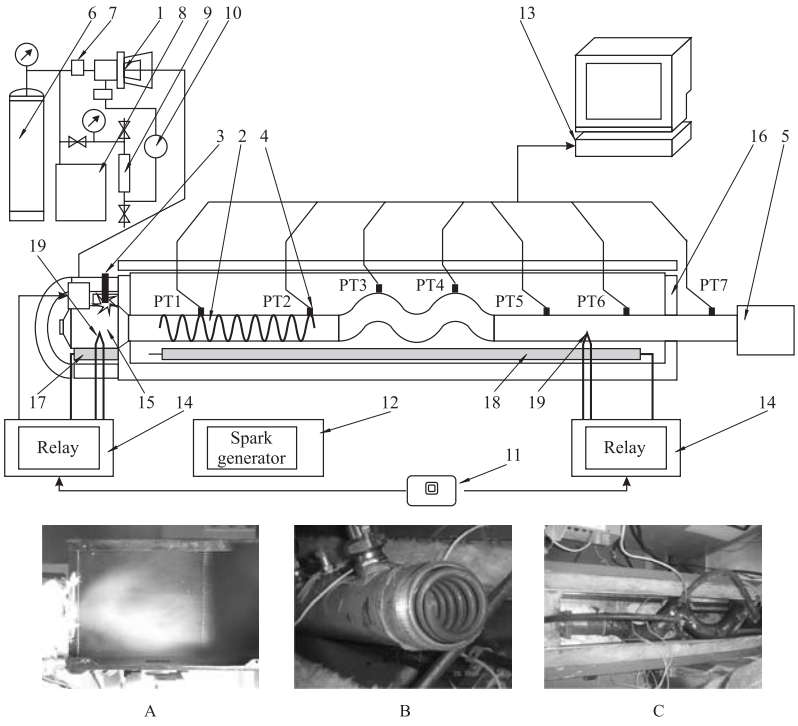

Figure 25: Shchematic of the experimental setup with a kerosene prevaporizer (A), Shchelkin spiral (B), and 2-coil tube section enhancing fast DDT (C)

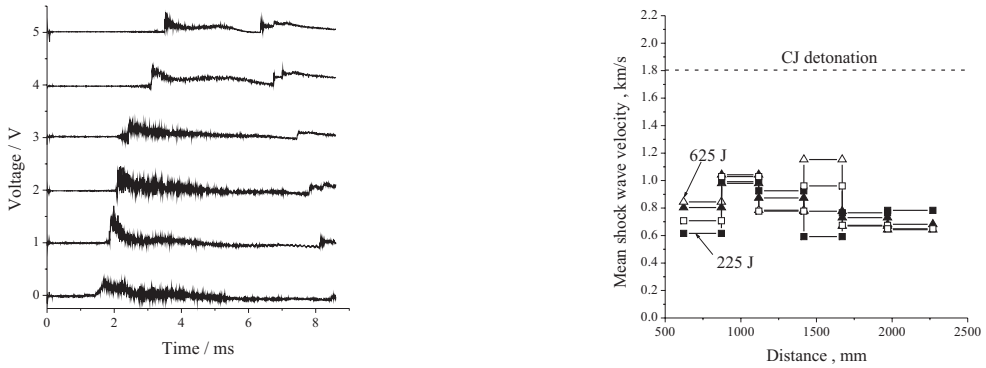

(*a*) (*b*)

Figure 26: Pressure profiles recorded by transducers PT1–PT6 in an experiment with an ignition energy of E = 225 J (*a*), and the measured shock wave velocities in a two-phase mixture of aviation kerosene with air over different measurement segments at different ignition energies (*b*)

was 120–130°C and the temperature of the tube segment up to pressure transducer PT6 was 110–120°C. The temperature of the tube segment downstream from pressure transducer PT6 was 20–30 C. The fuel–air mixture was ignited in the prevaporizer either by a standard spark plug or by the three-electrode discharge.

In the experiments with the straight tube the ignition energy was varied from 5 to 700 J. The maximum registered shock wave velocity in the straight tube was about 1200 m/s (Fig. 26).

The second experimental series was performed with the 2-coil tube segment. This tube segment consisted of two complete turns of the tube with the external diameter of 57 mm tightly around a rod 28 mm in diameter with the pitch of 255 mm. The curved tube segment was mounted 100 mm downstream from the end of the Shchelkin spiral. The ignition energy was varied from 5 to 176 J. In these experiments, we have repeatedly registered fast DDT and detonations even at the lowest ignition energy used (5 J). Figure 27*a* shows the example of pressure records by pressure transducers PT1 to PT7 at the ignition energy of 5 J indicating the fast DDT with the onset of detonation between transducers PT5 and PT6. Figure 27*b* shows the measured shock wave velocities along the detonation tube in 12 runs with the ignition energy ranging from 5 to 130 J. Clearly, fast DDT in aviation kerosene – air mixture was repeatedly attained at a distance of about 2 m even at an ignition energy of 5 J. This effect should be solely attributed to the use of the curved tube segment.

To further decrease the ignition energy we have designed and fabricated a flame-jet igniter operating on the principle of a classic prechamber with a standard automobile spark plug. The igniter operating on a two-phase gasoline A80 (Octane number 80) – air mixture was attached to the detonation tube of Fig. 25 instead of the prevaporizer. Before ignition, the tube was purged by the two-phase mixture issuing through the igniter nozzle. Spark ignition of the mixture in the igniter (ignition energy of about 100 mJ) resulted in the energetic flame jet issuing through the igniter nozzle (Fig. 28*a*). As follows from Fig. 28*b*, this flame jet is capable of initiating a detonation via fast DDT in the 2-coil tube segment. Clearly, the concept of flame-jet ignition offers a promising way of decreasing the detonation ignition energy down to fractions of Joule. The total time from mixture ignition in the flame-jet igniter

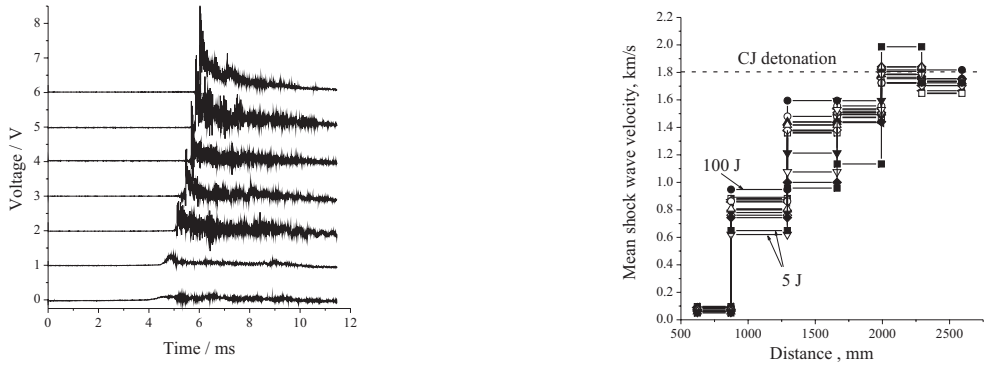

(*a*) (*b*)

Figure 27: Pressure profiles recorded by transducers PT1–PT7 in an experiment with an ignition energy of $E = 5$ J (*a*), and the measured shock wave velocities in a two-phase mixture of aviation kerosene with air over different measurement segments at different ignition energies (*b*)

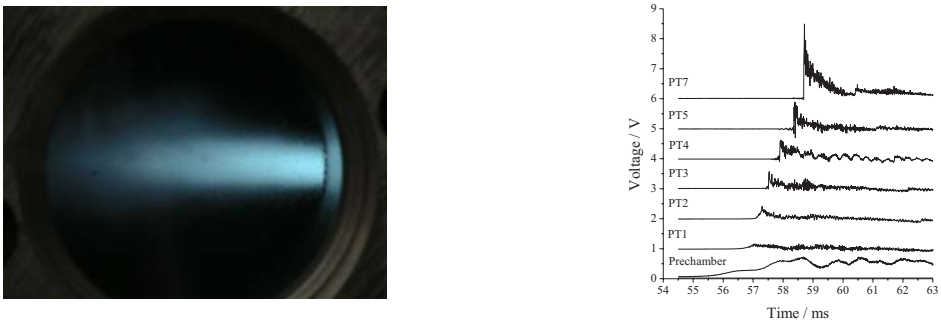

(*a*) (*b*)

Figure 28: Flame jet issuing from the igniter nozzle at ignition energy of 100 mJ (*a*) and pressure profiles recorded by transducers PT1–PT7 and a transducer located in the prechamber for the experiment with liquid gasoline A-80 – air mixture at ignition energy of $E = 100$ mJ (*b*)

to detonation initiation was about 10.5 ms. The time taken for the fast DDT to occur after flame jet entering the detonation tube was about 5–6 ms.

4. Concluding remarks

This paper is focused on the author's recent experimental studies of direct initiation of confined detonation and DDT in hydrocarbon fuel sprays and drop suspensions in air. In the experiments on direct initiation of heterogeneous *n*-hexane and *n*-heptane – air detonations by electric igniters in straight round tubes of different diameters a critical initiation energy was obtained. The critical initiation energy appeared to be a function of the characteristic time of energy deposition by the electric discharge, igniter location in the spray, and tube diameter. It has been shown that a nearly two-fold decrease in tube diameter (from 51 to 28 mm) resulted

in decreasing the critical initiation energy from 1.5 to 0.82 kJ for both *n*-hexane and *n*-heptane – air detonations. The use of two successively triggered electric igniters for direct detonation initiation in heterogeneous *n*-hexane and *n*-heptane – air mixtures was shown to result in further nearly two-fold decrease of the critical initiation energy. It has been demonstrated experimentally that for obtaining a spray detonation with two successively triggered igniters some resonant conditions have to be met in terms of shock wave arrival time and time delay of igner triggering. The detonation peninsula at the "initiation energy vs. triggering time delay" plane was shown to be very narrow which is the indication of the necessity to carefully synchronize successive triggering of the igniters.

Several experimental examples illustrating the occurrence of fast DDT were also presented. Fast DDT was shown to occur under conditions when, in a flow of an explosive mixture, self-ignition zones behind a relatively weak shock wave can be formed synchronously with the running wave. Such zones can be formed because of reflections of the wave from curved surfaces in bends, tube coils, etc. It was shown experimentally that the critical velocity required for fast DDT can be fairly low, about 800 m/s. Such shock waves can be readily obtained in straight tubes with rough inner surfaces, regular obstacles in the form of Shchelkin spirals or orifice plates at a fairly low ignition energy. On the one hand, various combinations of tube elements (and ignition sources) resulting in the formation of shock waves propagating at a velocity higher than 800 m/s with coils, bends, local obstacles, etc., should be considered potentially dangerous. In designing explosion-proof works, such combinations should be avoided. The possibility of fast DDT therefore poses fundamental problems of conditions of their occurrence and precautions that should be taken to prevent them. On the other hand, the combinations considered offer much promise for fast initiation of detonation, for instance, in pulsed detonation engines [39]. Further research is needed to gain better understanding of the accompanying phenomena.

Acknowledgments

I would like to thank P. Rambaud and C. O. Asma of the Aeronautic and Aerospace Department of the Von Karman Institute (VKI) for the kind invitation to take part in the VKI Lecture Series "Liquid Fragmentation in High Speed Flow" and present this paper. Also, I gratefully acknowledge the contribution of my colleagues V. S. Aksenov and V. Ya. Basevich for their valuable contribution to the experimental studies described in this paper.

References

1. Roy G.D., Frolov S.M., Borisov A.A., Netzer, D.W., Prog. Energy Comb. Sci., 2004, 30(6), 545.
2. Frolov S.M., Barykin A.E., and Borisov A.A., Rus. J. Cjem. Phys., 2004, 23(3), 17.
3. Mitrofanov, V. V., Pinaev, A. V. and Zhdan, S. A., Acta Astronautica, 1979, 6(3/4), 281.
4. Zhdan S. A., J. Combustion, Explosion, Schock Waves, 1981, 17(6), 105.
5. Zhdan, S. A., Detonation waves in gas-droplet systems upon explosion of a cylindrical charge, Abstracts of the 8th ICDERS, Minsk, USSR, , 1981, 50.
6. Voronin D. V. and Zhdan S. A., J. Comb., Explos., Shock Waves, 1984, 20(4), 112.
7. Vasil'ev A. A., Zhdan S. A. and Mitrofanov V. V., In: Gaseous and Heterogeneous Detonations: Science to Applications, G. D. Roy, S. M. Frolov, K. Kailasanath and N. N. Smirnov (Eds.), Enas Publ., Moscow, Russia, 1999, 25.
8. Dabora E.K., In: Progress in Astronautics and Aeronautics , New York: AIAA, 1991, 133, 311.

9. Dabora E.K., Ragland K.W., and Nicholls J.A., Astronaut. Acta, 1966, 12(1), 9.
10. Benedick W.B., Tieszen S.R., Knystautas R., and Lee J.H.S., In: Dynamics of Detonations and Explosions, New York: AIAA, 1991, 133, 297.
11. Nicholls J. A., Bar-Or R., Gabrijel Z., et al., AIAA J., 1979, 288, 4.
12. Borisov A. A., Private communications.
13. Zel'dovich Ya. B., Kogarko S. M. and Simonov N. N., Sov. J. Technical Physics, 1956, 26(8), 1744.
14. Frolov S. M., Basevich V. Ya., Aksenov V. S. and Polikhov S. A., In: Advances in Confined Detonations, G. Roy, S. Frolov, R. Santoro and S. Tsyganov (Eds.), Torus Press, Moscow, 2002, 150.
15. Frolov S. M., Basevich V. Ya., Aksenov V. S., and Polikhov S. A., J. Propulsion Power, 2005, 21(1), 54.
16. Frolov S. M., Basevich V. Ya. and Aksenov V. S., Proc. 14th ONR Propulsion Meeting, G. D. Roy and F. Mashayek (Eds.), University of Illinois at Chicago, Chicago, IL, 2001, 202.
17. Frolov S. M., Basevich V. Ya., and Aksenov V. S., J. Shock Waves, 2005, 14(3), 175.
18. Bone W. A. and Fraser R. P., Philos. Trans. R. Soc. London, Ser. A, 1929, 228, 197.
19. Zel'dovich Ya. B., Theory of Combustion and Detonation of Gases, Akad. Nauk SSSR Publ., Moscow, 1944.
20. Shchelkin K. I., Fast Combustion and Spin Detonation of Gases, Voenizdat Publ., Moscow, 1949.
21. Oppenheim A. K., Introduction to Gasdynamics of Explosions, Springer, Wien, 1972.
22. Lee J. H. S. and Moen I., Prog. Energy Comb.. Sci., 1980, 6, 359.
23. Higgins A. J., Pinard P., Yoshinaka A. K., and Lee J. H. S., In: Pulse Detonation Engines, Ed. by S. M. Frolov, Torus Press, Moscow, 2006, 65.
24. Frolov S. M., Basevich V. Ya., Aksenov V. S., and Polikhov S. A., J. Propulsion Power, 2003, 19 (4), 573.
25. Frolov S. M., Basevich V. Ya., Aksenov V. S., and Polikhov S. A., Dokl. Phys. Chem., 2004, 394(1), 16.
26. Frolov S. M., Basevich V. Ya., Aksenov V. S., and Polikhov S. A., Rus. J. Chem. Phys., 2004, 23(4), 61.
27. Frolov S. M., Basevich V. Ya., Aksenov V. S., and Polikhov S. A., Dokl. Phys. Chem., 2004, 394(2), 39.
28. Frolov S. M., J. Loss Prevention, 2005, 19(2–3), 238.
29. Frolov S. M., J. Propulsion Power, 2006, 6, 1162.
30. Basevich V.Ya., Frolov S.M., and Posvyanskii V.S., Rus. J. Chem. Phys., 2005, 24(7), 58.
31. Peraldi O., Knystautas R., and Lee J. H. S., Proc. Combust. Inst., 1986, 21, 1629.
32. Basevich V. Ya., Vedeneev V. I., Frolov S. M., and Romanovich L. B., Rus. J. Chem. Phys., 2006, 25(11), 87.
33. Webber W. T., Proc. 8th Sympos. (Intern.) on Combustion, Williams and Wilkins, Baltimore, 1960.
34. Borisov A. A., Gelfand B. E., Gubin S. A., Kogarko S. M. and Podgrebenkov A. L., Sov. J. Appl. Mech. Techn. Phys., 1970, 1, 163.
35. Borisov A. A., Gelfand B. E., Gubin S. A., Kogarko S. M. and Podgrebenkov A. L., Doklady USSR Acad. Sci., 1970, 190(3), 621.
36. Pierce, T. N. and Nicholls, J. A., Astronaut. Acta, 1972, 17(4–5), 703.
37. Frolov S.M., Aksenov V. S. Dokl. Phys. Chem., 2005, 401(1), 28.
38. Frolov S.M., Aksenov V. S. Dokl. Phys. Chem., 2007, 416(1), 261.
39. Frolov S. M., Ed. Pulse Detonation Engines, Torus Press, Moscow, 2006.